Hindawi
Geofluids
Volume 2022, Article ID 6408714, 11 pages
https://doi.org/10.1155/2022/6408714

Research Article

Analysis of Thermal Environment and Its Influencing Factors in Deep Stope of Metal Mine

Shuang You[1,2], **Jincui Sun**[1,2], **Hongguang Ji**[1,2] **and Qixing Feng**[1,2]

[1]*School of Civil and Resource Engineering, University of Science and Technology Beijing, Beijing 100083, China*
[2]*Beijing Key Laboratory of Urban Underground Space Engineering, University of Science and Technology Beijing, Beijing 100083, China*

Correspondence should be addressed to Jincui Sun; sunjincui0922@163.com

Received 17 April 2022; Accepted 21 May 2022; Published 3 June 2022

Academic Editor: Peng Hou

In order to scientifically evaluate the thermal environment of the deep stope and its influencing factors, research was conducted on the thermal environment in Sanshandao Gold Mine, the theoretical calculations and structural analysis of heat release from 8 types of heat sources in the three sub-levels of -930 m, -945 m, and -960 m were carried out, and quantitative characterization was made on the influential degree of comprehensive heat release on the thermal environment, and it was clear that the heat release from the surrounding rock and mechanical and electrical equipment were the main parts at the deep mining site and the proportion of heat release from other heat sources is basically stable. Then, through the analysis of the influence factors of heat sources in the mining site, 17 evaluation indexes of the influence factors of the mining site thermal environment were sorted out, and the indexes' weight was calculated based on the entropy weighting method, and it was learned that the largest weight of the influence on the thermal environment factors in a single excavation working face was the water gushing in the roadway. The TOPSIS method was used to comprehensively analyze and rank the thermal damage degree in the three middle sections. The results show that the degree of thermal damage in the -960 m is more severe than that in the -930 m and -945 m. This will provide some basic basis for the evaluation and prevention of thermal damage in deep mining projects, and is of great significance for improving mine production efficiency.

1. Introduction

Deep mining is the inevitable trend of future development of mining industry in China and even the world [1]. The temperature of the working face in a mine with a depth of more than 1,000 meters is close to the extreme temperature of human survival, and the relative humidity reaches 100%. The thermal environment of the stope induces a sharp increase in the fatigue and irritability of the miners [2]. According to the "Control Of Mine Victims," every 1°C of ambient temperature in the mine exceeding the standard will lead to a decrease of 7% to 10% in the labor efficiency of miners [3]. When the temperature is too high, it will threaten the safety of personnel and seriously hinder the production efficiency of the mine [4]. By calculating the heat released by common heat sources and comprehensively analyzing various indicators of thermal environment, scientifically evaluating the thermal environment of deep stope engineering is of great significance for safe mining in deep engineering [5–7].

In recent years, extensive research on thermal environment evaluation mainly includes the theoretical analysis of high-temperature heat damage factors and the establishment of evaluation models [8]. By studying heat stress indicators such as WBGT, HIS, and effective temperature, Park et al. [9] determined the impact of different heat stress indicators on the thermal environment; Wang et al. [10] used the "expert consultation method" to determine the evaluation indicators, and used the relative importance sequence matrix method to obtain the weight of each indicator; Gao et al. [11] et al. studied the evaluation of mine environment comfort, deduced an optimal combination weighting model based on the least squares method, and proposed a new method to determine the

weight of the evaluation indicator of mine environment comfort; Zhao et al. [12] defined the main influencing factors of thermal environment assessment and by comparing the difference in standard score and standard deep thermal environment parameters to determine the severity of thermal stress; SL A et al. [13] extended ORESTE with hybrid evaluation information to solve the noncompensation problems of the indexes and found a suitable method for evaluating the thermal comfort in underground mines; Zhang et al. [14] analyzed the factors affecting the thermal comfort of miners and the human body heat exchange model and established an index system of calculation theory to effectively evaluate the thermal environment of the mine; Ryan Anderson and Souza [15] continuously monitored and captured environmental parameters at key locations in the mine, and studied the evaluation and management methods of heat damage; Zhou et al. [16] used ANSYS to numerically simulate the effect of cold airflow diffusion on the mine ambient temperature, and the research results provided a reference for the layout of ventilation pipes in high-temperature heat-damaged mine roadways; He and Xu [17] analyzed the heat damage characteristics of deep wells in Sanhejian, and adopted the HEMS system to provide a technical approach for deep well heat damage control, and turned deep well heat damage into resources; Nie et al. [18] optimized the deep mine ventilation system and proposed to build a cooling system with mine water as the cooling source to solve the problem of high-temperature heat damage in deep mines; Guo et al. [19] proposed that the thermal environment of the working face is closely related to the ventilation mode of the working face. Numerical research shows that the Y-shaped ventilation system can reduce the temperature and humidity of the surrounding environment more effectively than the U-shaped ventilation system. Summarizing the above research work on mine thermal environment assessment, it can be found that most of the research work is carried out on shallow stopes but not in deep well environment, and there are problems such as single evaluation index, incomplete heat source types, and strong subjectivity in determining weights.

Compared with the shallow stope, the calculation formula of heat released by each heat source in the deep stope, the evaluation method of influencing factors, and the proportion of heat released are different. In this paper, through the field investigation of the heat source in the mining process of Sanshandao metal mine, the theoretical calculation of the heat released by the stope heat source is carried out, the main composition and proportion of the underground heat load are analyzed, and the quantitative characterization is carried out by the change of the ambient temperature. The entropy weight method (EWM) was used to calculate the weights of heat source influence indexes, and the TOPSIS method was used to predict the stope heat damage degree in three deep sub-levels. The research results will be of great significance to improve the underground working environment, prevent heat damage, protect the safety of operators, and improve mine production efficiency.

2. Characterization, Indexes, and Basic Parameters of Thermal Environment in Deep Stope

2.1. Composition of Thermal Environment System in Deep Stope. The thermal environment of the deep stope refers to the temperature environment of deep mine. The air temperature and humidity in deep mine are high, so temperature and humidity are the two main aspects to describe the thermal comfort. This paper is to study the thermal environment of stope heading face in the Sanshandao deep mine, through on-site research and investigation, the working face humidity of deep stope is almost 100%, so this paper is aimed to analyze the impact of heat released on the stope thermal environment and evaluation methods.

The thermal environment of deep mine is affected by a variety of factors, and each factor affects each other. Some heat release can be calculated by statistical laws, while others cannot be directly quantified. For example, such factors as surface atmosphere have an important influence on the air flow temperature in the mine thermal environment [20]. Although the contribution rate of surface atmosphere to heat release in the mine thermal environment cannot be obtained, the influence weight of underground airflow temperature can be calculated, and the underground airflow temperature is also one of the indispensable indexes in calculating surrounding rock heat release.

The influence factors of thermal environment temperature changes in deep mines (see Figure 1) can be divided into two categories according to heat transfer methods. One is relative heat sources, including surrounding rock and underground water. The heat release of such heat sources is closely related to the ambient temperature of the stope. The other type is absolute heat source, including air compression heat release, electromechanical equipment heat release, and blasting heat release. The heat release of this type is less affected by the ambient temperature. Based on the comprehensive investigation results, the main heat sources in deep mine are surrounding rock heat release, underground water heat release, air compression heat release, electromechanical equipment heat release, ore transport process heat release, hydration heat release of the filling body, personnel heat release, and blasting heat release. In this paper, these 8 types are defined as the first-level index factors of thermal environment evaluation, and the parameters affecting the first-level index are defined as the second-level index factors.

2.2. Research on Basic Parameters of Stope. Through in situ investigation and analysis of the basic parameters of the deep mining face in Sanshandao, it can be seen from Table 1 that along the depth direction of -930 m to -960 m, the temperature of the roadway wall does not change significantly, while the ventilation volume and wind speed of roadway increase significantly as the depth increases. In addition, it can be found that the roadway total length and the working face width are also significantly different in different sub-levels. It can be seen from Table 2 that the trolleys' power is much smaller than that of the scrapers and trucks. The three trucks' power accounts for 54% of total power of

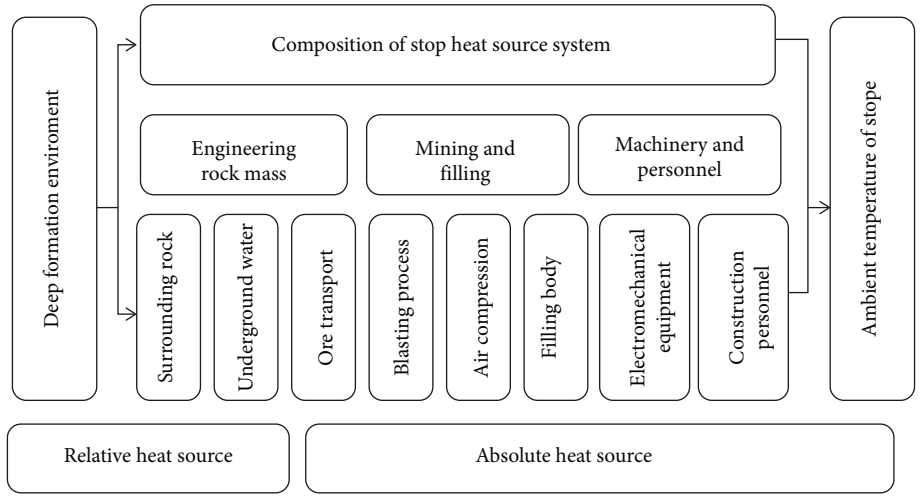

Figure 1: Schematic diagram of heat source system in deep mine stope.

Table 1: Parameters of heading face.

Depth/m	Ventilation quantity/$m^3 \cdot s^{-1}$	Wind temperature/°C	Roadway wall temperature/°C	Wind speed/$m \cdot s^{-1}$	Total length of roadway/m	Working face width/m
-930	15.16	25	30	1.0	180	3.6
-945	18.20	25	31	1.2	360	4.5
-960	22.53	22	31	1.6	645	4.0

Table 2: Electromechanical equipment parameters in each sub-level.

Equipment name	Equipment model	Power/kW	Number
Jumbo	DD311	70	1
Rock bolting jumbo	DS311	70	1
Shotcrete trolley	SPM4210	75	1
Scraper	ST3.5	136	1
Truck	—	136	3

electromechanical equipment. It can be seen from Table 3 that the initial and final temperatures of the water in the three sub-levels are the same, but the water inflow in the sub-level of -960 is much larger than that in the other two sub-levels. After investigation, it was found that there was a slump in the sub-level, and during the mining process, water would be drained to the sub-level. Therefore, the heat release of groundwater in the -960 sub-level is also much higher than that of the other two sub-levels. It can be seen from Table 4 that in the different sub-level, the daily amount of ore mined is also different, and the ore transportation distance tends to increase with the increase of the sub-level depth. This is because the greater the depth, the worse the stope environment and the more complex mining conditions, resulting in a reduction in the amount of ore mined and a corresponding increase in the transportation distance. It can be seen from Table 5 that the daily gunpowder consumption of the -930 sub-level is much more than the other two sub-levels, so the blasting heat release of this sub-level is the largest. However, the surface area of the filling body of

Table 3: Groundwater parameters.

Depth/m	Water inflow/$m^3 \cdot h^{-1}$	Initial temperature of water/°C	Final temperature of water/°C
-930	3	42	39
-945	3	42	39
-960	20	42	39

Table 4: Personnel and ore extraction parameters.

Depth/m	The number of worker at work location	Daily ore output/t	Ore transportation distance/m
-930	8	200	200
-945	10	120	360
-960	6	150	600

Table 5: Other relevant parameters.

Depth/m	Daily gunpowder consumption/$kg \cdot d^{-1}$	Fill body surface area per fill/m^2	The vertical depth of the downward flow of the wind/m
-930	144	260	30
-945	72	300	15
-960	96	600	45

the -930 sub-level is much lower than that of the other two sub-levels, so the hydration heat release of the filling body is the smallest in this sub-level.

3. Calculation and Analysis of Heat Release from Heat Source in Deep Stope

3.1. Calculation of Heat Released from Heat Source in Deep Stope. The heat release from the surrounding rock is one of the main heat sources in deep stope, and its heat release form is heat conduction. As depth increases, the temperature of the surrounding rock also increases. In the early stage of roadway excavation, heat exchange occurs between high-temperature surrounding rock on the roadway wall and wind flow, resulting in a gradual increase in the temperature of the wind flow. Over time, the temperature difference between the two gradually decreases, and the heat release of the wall facing the wind flow tends to be stable. The calculation formula is

$$Q_{wy} = k_\tau LU\left(t_{cs} - t_{pj}\right), \tag{1}$$

where k_τ is the unstable heat exchange coefficient between surrounding rock and wind flow, kW/(m^2·°C), which is taken as 0.5; U is the perimeter of the roadway, m; L is the length of the single excavation working face, which is taken as 5 m; t_{cs} is the initial temperature of the surrounding rock, °C; t_{pj} is the average temperature of the wind flow in the roadway, °C.

The heat release from groundwater - in the process of deep well mining, the phenomenon of water gushing is common. Because the specific heat capacity of water is very high, when the water gushing phenomenon occurs in the working face, a large amount of high-temperature groundwater will release a lot of heat to the surroundings, resulting in the ambient temperature rise immediately. In the local working area, the large amount of high-temperature water inflow is one of the important factors leading to heat damage. According to the principle of thermodynamics, the amount of water inflow in the roadway and the initial and final temperature of the water can be used to calculate the heat release of water. The calculation formula is as follows (2)

$$Q_w = M_w c_w (t_{wH} - t_{wK}), \tag{2}$$

where M_w is the water inflow in the roadway, kg/h; c_w is the specific heat capacity of water, 4.1868 kJ/(kg·°C); t_{wH} and t_{wK} are the initial and final temperature of water, °C. The initial temperature of the water is the temperature measured at the time of water gushing during the mining process, and the final temperature of the water is the temperature when the water enters the drainage system at the end of the mining per unit of mining length.

The heat release from air compression is that in the process of deep well production, when the air flows down the wellbore, its pressure and temperature will rise, resulting in the compression of the volume and the release of heat. Physically speaking, the self-compression of the mine air flow does not form a thermal field, but it is an important factor affecting the thermal state of the mine air flow. Especially for deep mines, the heat released by the air self-compression is quite large, so this paper takes it as a heat source. The formula for calculating the heat released from air compression is:

$$Q_{\text{air}} = GA \cdot \Delta Z \cdot E, \tag{3}$$

where G is air mass flow, kg/s; A is equivalent of air thermal work conversion, which is taken as 9.81×10^{-3} kJ/kg·m; $\triangle Z$ is the difference between the air flow inlet elevation and the lowest air flow elevation, m; E is the coefficient of compression heat absorbed by the air flow, ≤1. Generally, the heat balance calculation method of air compression heat and the convection heat transfer on borehole wall is adopted, so the value of E is 1.

The heat release from electromechanical equipment - with the improvement of mechanization level of production links such as excavation, stopping, and transportation during mining, the power of electromechanical equipment has increased significantly. A considerable part of the electrical energy consumed by electromechanical equipment is converted into heat energy and released into the surrounding medium. If the heat released by the equipment cannot be discharged in time in the local area, the temperature of the area will rise rapidly, and the heat damage will be aggravated, which will have an adverse effect on the production of the local working face. Especially in deep mines with large mining scale and high degree of mechanization, the heat release from electromechanical equipment has become one of the important causes for heat damage in deep mines that cannot be ignored. The heat release from electromechanical equipment can be calculated according to formula (4):

$$Q_e = \sum_{i=1}^{n} (1 - \eta_i) N_i, \tag{4}$$

where η is the efficiency of electromechanical equipment, %; when the electromechanical equipment does work in the horizontal roadway, η=0; N is the power of the equipment, kW.

The heat release during the ore transportation is due to the large difference between the temperature of the mined ore and the air flow temperature. In addition, the ore is in a flat state during the transportation process, and has a wide contact area with the air, resulting in a large heat exchange between the ore and the air flow, which makes the air in the stope rise rapidly. Therefore, this paper considers it as a single heat source for calculation. The heat release of ore during transportation can be calculated according to formula (5):

$$Q_{ys} = mc_m \Delta t, \tag{5}$$

where m is the transport amount of ore, kg/s; c_m is the specific heat capacity of ore, kJ/(kg·°C); $\triangle t$ is the temperature difference between ore and air, °C, which can be determined

by formula (6):

$$\Delta t = 0.0024 L_k^{0.8} \left(t_p - t_{wm}\right), \tag{6}$$

where L_k is transport distance, m; t_p is the average temperature of the ore during transportation, °C; t_{wm} is the average wet bulb temperature of the air flow in the transport tunnel, °C.

The hydration heat release of the filling body is for high-temperature mines that use the filling method. In order to support the two sides of rocks in the goaf, and to continue the upper layered stopping to form a base plate to stand on, the filling is performed. During the cementation process of the filling material, a certain amount of heat is precipitated, which is emitted into the stope interior through the air. The hydration heat release of the filling body refers to the hydration heat release of concrete, and the calculation formula for the heat release is as follows:

$$Q_s = K_s M_s, \tag{7}$$

where K_s is the heat release per unit area of concrete hydration, generally taking 0.015~0.016 kW/m^2; M_s is the filling body surface area for each filling, m^2.

The personnel heat release is the heat released by stope workers to the surrounding environment. Although the proportion of human body heat release is smaller than that of other heat sources, the density of workers at the excavation working face is relatively large. At this time, the effect of personnel heat release on air flow temperature cannot be ignored. The main determinants of personnel heat release are the labor intensity of personnel and the time of continuous operation, which can be calculated according to formula:

$$Q_{\text{man}} = nq, \tag{8}$$

where q is the per capita heat release, which is 0.275kw/person; n is the number of worker in the working face.

The blasting heat release is the heat released when metal mines use blasting to mine. The heat generated by the explosion of the explosive is released instantaneously and has double exothermic properties, which plays a leading role in the short-term increase of the stope air temperature. A part of the heat is rapidly released to the air and surrounding rock during blasting, forming a local heat source with high temperature instantly; the other part is stored in the surrounding rock in the form of heat energy, which will be gradually released into the surrounding air over a long period of time. The formula for calculating the heat of explosion is as follows:

$$Q_b = 0.14 G_h, \tag{9}$$

where G_h is the daily average gunpowder consumption at the operation site, kg/d.

3.2. Analysis of Heat Release Structure of Stope Heat Source. According to the above formulas (1)–(9), calculate the heat release of each heat source in different sub-levels of deep well, as shown in Table 6. Draw a histogram of the proportion of heat released by each heat source in each sub-level according to the summary table of heat released by each heat source, as shown in Figure 2.

Figure 2 shows the contribution rate of heat released by different heat sources in the sub-level of the Sanshandao Metal Mine. The heat released by the surrounding rock and the heat released by the electromechanical equipment are the two main sources of heat, accounting for about 80%-90% of the total heat release; it can be seen from Table 6 that with the increase of the depth of the sub-level, the heat released by the surrounding rock tends to increase, and the heat release of the surrounding rock is the most important downhole heat source in each sub-level. However, due to the difference of total heat release in each sub-level, the heat release ratio of surrounding rock in the three sub-levels in Figure 2 shows a jump change, resulting in the proportion of heat released by surrounding rocks in the sub-level of -960 m is lower than that of the sub-level of -945 m; the proportion of heat released by electromechanical equipment shows a law of decreasing segment by segment, but the number and power of electromechanical equipment in each middle segment are the same. This is mainly because the total heat release of each middle segment is different, which leads to changes in the proportion of heat released by electromechanical equipment. Due to the sudden increase of groundwater outflow in the sub-level of -960 m, the heat release of groundwater is significantly higher than that of the other two sub-levels; generally speaking, the proportion of personnel heat release is the smallest, and can even be ignored. However, due to the particularity of human nature, any stage of mining is accompanied by personnel cooling, so it is regarded as a necessary heat source.

When carrying out heat damage prevention and control work, the main heat release sources in different stopes should be identified, and targeted measures should be formulated. The heat transfer efficiency of surrounding rock is reduced by spraying insulating material on the rock wall to form a protective layer to solve the heat release problem of surrounding rock. A reasonable independent ventilation system should be set up in the electromechanical chamber, and the wind path length should be shortened as far as possible to solve the heat release problem of mechanical equipment; the heat release problem of groundwater can be solved by laying thermal insulation pipelines in the return air section and implementing advanced hydrophobic measures when pumping and draining underground hot water. The technical means to solve the heat release problems of other heat release sources are mainly to adjust the ventilation system to discharge heat to the outside of the stope as soon as possible, such as speeding up the air flow speed, reducing the air flow temperature, and increasing the air flow quality and other measures.

3.3. A Characterization Method for the Effect of Heat Release from Stope Heat Source on Thermal Environment. The influence of each heat source on the stope ambient temperature is quantitatively characterized by calculating the change in the average temperature of the stope thermal environment

Table 6: Summary of heat release (kW).

Depth/m	Surrounding rock	Groundwater	Air compression	Electromechanical equipment	Ore transportation	Filling body hydration	Personnel	Blasting	Total
-930	177.50	10.50	5.23	124.60	2.31	4.16	2.20	20.16	346.66
-945	240.00	10.50	3.14	124.60	2.59	4.80	2.75	10.08	398.46
-960	337.50	69.78	11.79	124.60	7.65	9.60	1.65	13.44	576.01

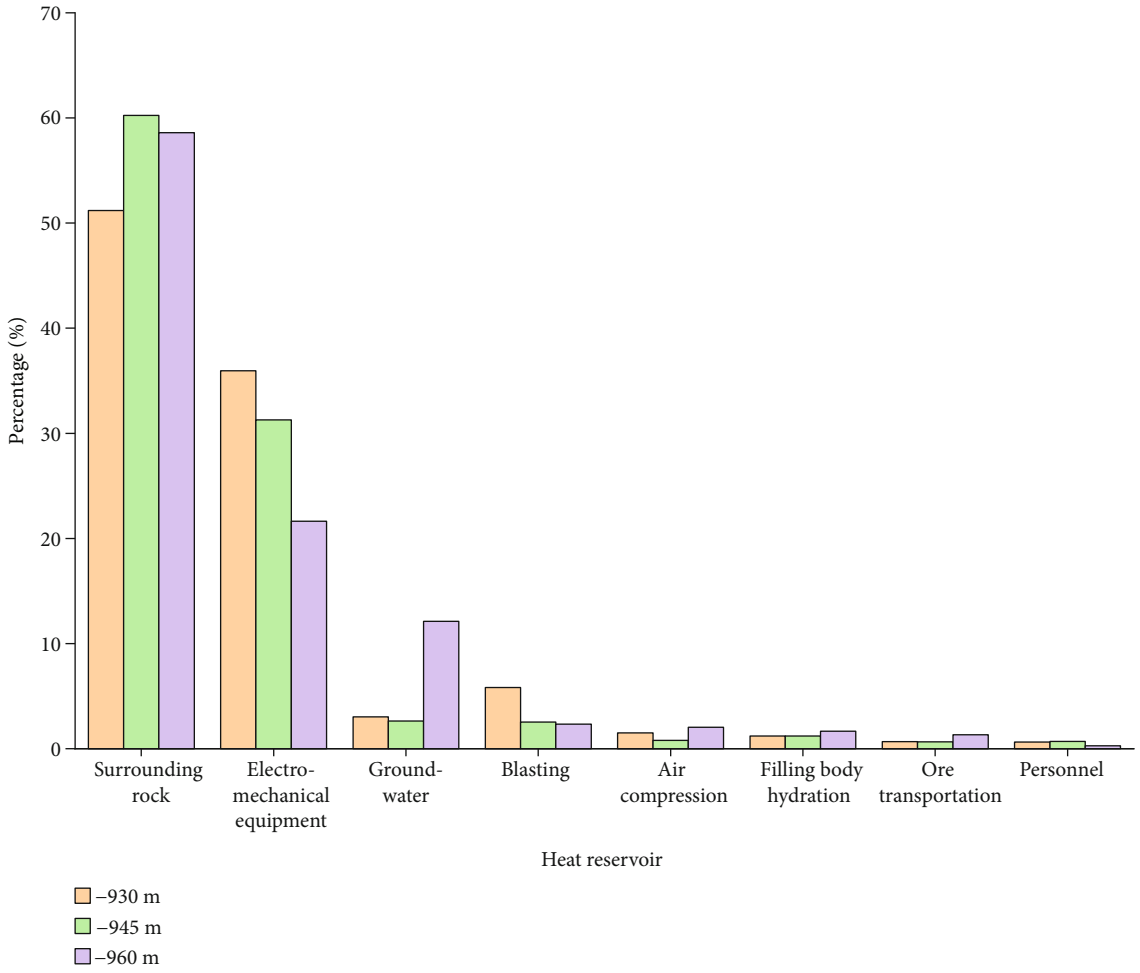

Figure 2: Heat release ratio of various heat sources in each sub-level.

caused by the total heat release. The formula is as follows

$$\Delta t = Q/c_{\text{air}} m_{\text{air}}, \tag{10}$$

where $\triangle t$ is ambient temperature change, ˚C; Q is total heat release, kW, $Q = Q_{wy} + Q_w + Q_{\text{air}} + Q_e + Q_{ys} + Q_s + Q_{\text{man}} + Q_b$; c_{air} is specific heat capacity of air, kJ/(kg·˚C). According to the "Handbook of Thermophysical Properties of Materials Commonly Used in Engineering"(15241·93), within the ambient temperature range of the deep stope, take the specific heat capacity of air under 1 standard atmosphere of 1.4 kJ/(kg·˚C); m_{air} is the mass flow of ambient air in the stope, kg·s^{-1}, $m_{\text{air}} = V_{\text{air}}\rho$, V_{air} is volume flow of ambient air in the stope, m^3·s^{-1}. It is difficult to obtain its stable value because of the large difference of air volume flow at different mining stages and locations in stope; ρ is air density, kg·m^{-3}, and the value is related to temperature and pressure in the stope.

4. Multi-Index Comprehensive Evaluation of Thermal Environment Based on EWM-TOPSIS Method

4.1. Determine the Weight of Thermal Environment Indicators. Entropy is a measure of uncertainty. Using the entropy weight method (EWN) to determine the weight of each evaluation index can effectively reduce the influence of human subjective factors on the weight. Based on this, this paper uses EWN to calculate the thermal environment index weight.

Table 7: Weight calculation and ranking of deep stope thermal environment indicators.

Secondary indicators	Entropy	Weight
L— Length of excavation face, m	0.99974	0.00324
U— Perimeter of roadway, m	0.99963	0.00450
tcs— Initial temperature of surrounding rock, ˚C	0.99973	0.00335
tpj—Average temperature of air flow, ˚C	0.99953	0.00585
Mw—Water inflow, kg·h^{-1}	0.96698	0.40661
twH—Initial temperature of water, ˚C	0.99974	0.00324
twK—Final temperature of water, ˚C	0.99974	0.02401
G—Mass flow of air flow, kg·s^{-1}	0.99805	0.02401
△Z—Difference between air inlet and bottom elevation, m	0.99047	0.11733
η— Efficiency of electromechanical equipment, %	0.99974	0.00324
N— Power of electromechanical equipment, kW	0.99974	0.00324
n—The number of equipment	0.99974	0.00324
Cm—Specific heat capacity of ore, KJ/(kg·˚C)	0.99974	0.00324
△t—Temperature difference between ore and air, ˚C	0.98261	0.21416
Ms— Surface area of filling body during one-time filling, m^2	0.99139	0.10603
n—The number of worker at the working face	0.99726	0.03379
Gh—Daily gunpowder consumption, kg·d^{-1}	0.99499	0.06170

Firstly, define the thermal environment index system and evaluation unit in deep stope, and select the secondary index that affects the thermal environment temperature of the stope as the object of entropy weight method evaluation. According to the data actually collected, the evaluation object was set as three evaluation units (the third sub-level: -930 m, -945 m, -960 m) contained in Tables 1–5, a total of 17 evaluation indicators. The existing thermal environment evaluation index system includes the larger the better type index and the smaller the better type index. The larger the better type indexes include the mass flow of air flow and the efficiency of electromechanical equipment, while the smaller the better type indexes include the length of the working face, the perimeter of the roadway, the initial temperature of the surrounding rock, the average temperature of the air flow in the roadway, the water inflow in the roadway, the initial and final temperature of the water, the difference between the elevation of the air flow inlet and the elevation of the air flow at the bottom of the well, the power of electromechanical equipment, the number of equipment, the specific heat capacity of ore, the temperature difference between ore and air, the surface area of filling body during one-time filling, the number of worker on working face, and the daily average consumption of gunpowder at operating site.

The initial evaluation matrix is a matrix composed of evaluation units and evaluation indicators, including "m" evaluation objects and "n" evaluation indicators. The initial evaluation matrix is as shown in formula (11):

$$A = \left(a_{ij}\right)_{m\times n} = \begin{bmatrix} a_{11} & a_{12} & \cdots & a_{1n} \\ a_{21} & a_{22} & \cdots & a_{2n} \\ \vdots & \vdots & \ddots & \vdots \\ a_{m1} & a_{m2} & \cdots & a_{mn} \end{bmatrix}, \tag{11}$$

where A is preliminary evaluation matrix; a_{ij} is the n_i evaluation indicator of the m_j evaluation unit (i=1, 2, 3 …; j=1, 2, 3 …).

Standardize the matrix $\boldsymbol{A}$, that is, perform dimensional normalization on the evaluation indicators to eliminate the dimensional difference of different indexes of the evaluated object. Establish a standardized decision matrix, see formula (12):

$$b_{ij} = a_{ij} / \sqrt{\sum_{i=1}^{n} a_{ij}^2}. \tag{12}$$

According to the standardized decision matrix, calculate the information entropy, see equation (13).

$$E_j = -k \sum_{i=1}^{m} f_{ij} \ln f_{ij} m, \tag{13}$$

where E_j is the information entropy; k is the entropy coefficient, $k = 1/\ln m$; $f_{ij} = (1 + b_{ij}) / \sum_{i=1}^{m} (1 + b_{ij})$.

Calculate the weight of the corresponding indicator according to formula (14).

$$W_j = \left(1 - E_j\right) / \left(n - \sum_{j=1}^{n} E_j\right). \tag{14}$$

It can be seen from Table 7 and Figure 3 that among 17 evaluation factors in the Sanshandao mining area affecting the thermal environment in a single excavation working face, the most influential factor is the water inflow in the roadway, accounting for 0.41, followed by the temperature difference between the ore and the air, with a weight of

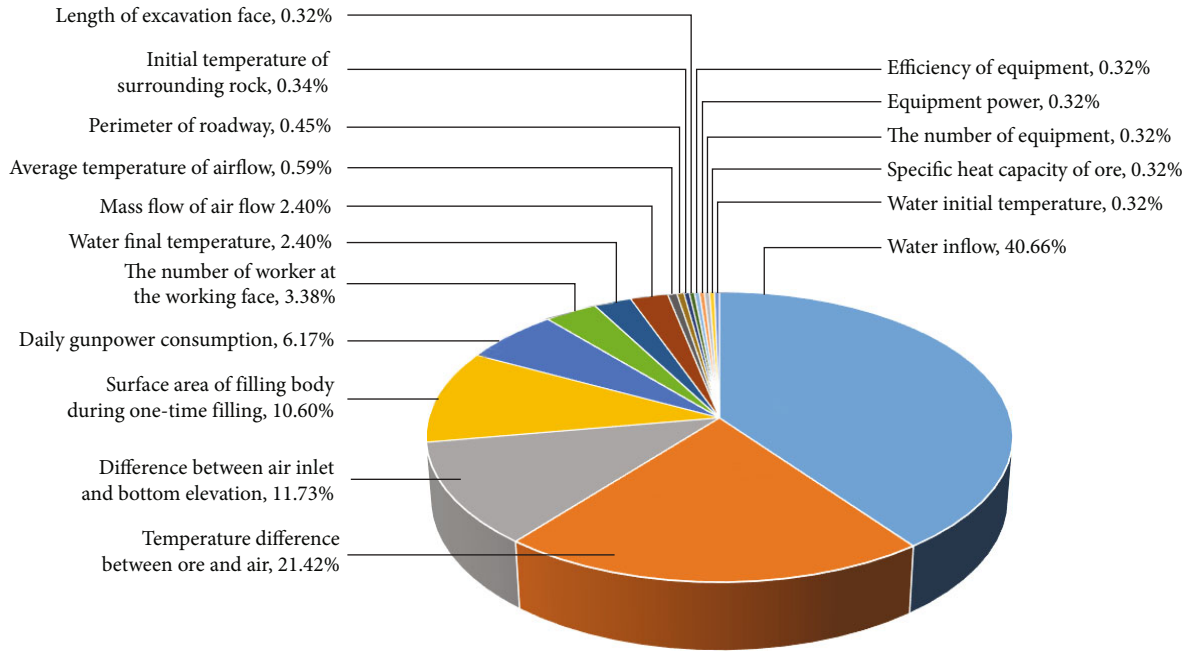

Figure 3: The pie chart of thermal environment indicators weight.

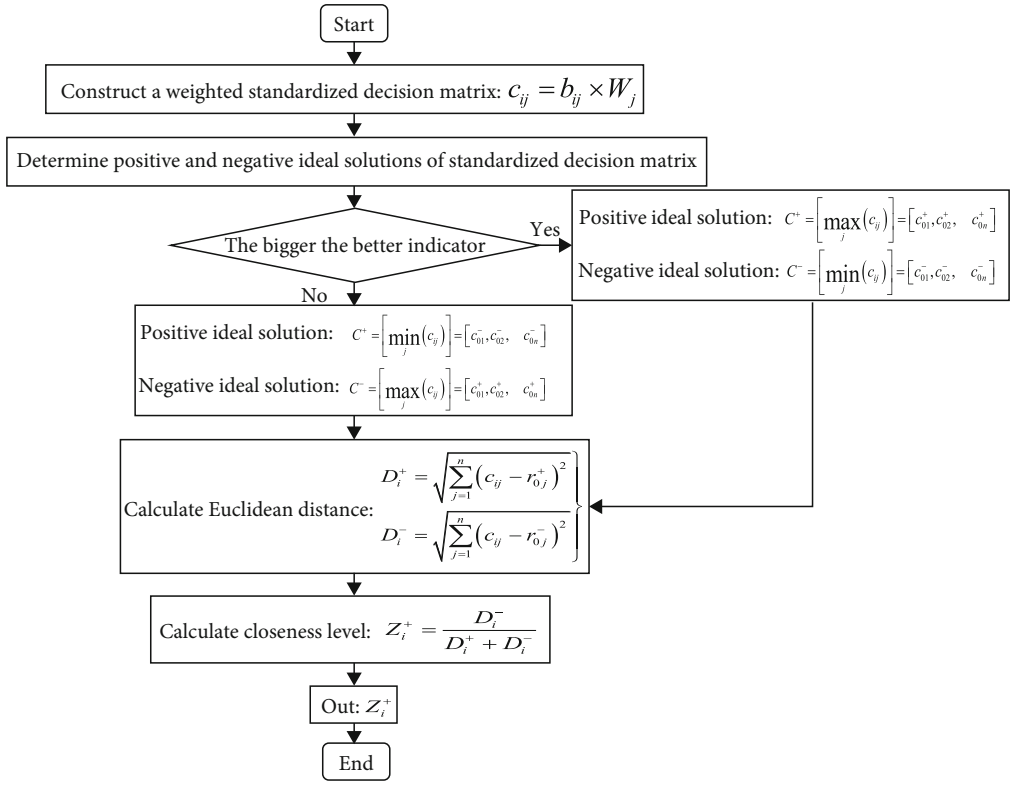

Figure 4: Stope heat damage evaluation based on entropy weight TOPSIS method process chart.

0.21. The order of weights of the remaining factors is the difference between air inlet and bottom well elevation, the surface area of the filling body during one-time filling, the daily gunpowder consumption at the operating site, the number of worker at the working face, the final temperature of the water, the mass flow of the air flow, the average temperature of air flow in the roadway, the perimeter of roadway, the initial temperature of surrounding rock, the initial temperature of water, the length of excavation face, the efficiency of electromechanical equipment, the power of electromechanical

Table 8: Weighted standardized decision matrix for each indicator.

(a)

Depth/m	Excavation face length	Roadway perimeter	Initial temperature of surrounding rock	Average temperature of air flow	Water inflow	Initial temperature of water	Final temperature of water	Mass flow of air flow	Distance between air inlet and bottom elevation
-930	0.00187	0.00247	0.00191	0.00351	0.05977	0.00187	0.01385	0.01107	0.06277
-945	0.00187	0.00273	0.00193	0.00351	0.05977	0.00187	0.01385	0.01330	0.03133
-960	0.00187	0.00259	0.00196	0.00309	0.39766	0.00187	0.01385	0.01666	0.09410

(b)

Depth/m	Efficiency of electromechanical equipment	Power of electromechanical equipment	The number of equipment	Specific heat capacity of ore	Temperature difference between ore and air	Surface area of filling body	The number of worker at the working face	Daily gunpowder consumption
-930	0.00187	0.00187	0.00187	0.00187	0.04369	0.03828	0.01913	0.04739
-945	0.00187	0.00187	0.00187	0.00187	0.08309	0.04421	0.02389	0.02147
-960	0.00187	0.00187	0.00187	0.00187	0.19253	0.08843	0.01433	0.03159

Table 9: Positive and negative ideal solutions of each indicator.

(a)

Indicator	Excavation face length	Roadway perimeter	Initial temperature of surrounding rock	Average temperature of air flow	Water inflow	Initial temperature of water	Final temperature of water	Mass flow of air flow	Distance between air inlet and bottom elevation
C^+	0.00187	0.00247	0.00191	0.00309	0.05977	0.00187	0.01385	0.01666	0.03133
C^-	0.00187	0.00273	0.00196	0.00351	0.39766	0.00187	0.01385	0.01107	0.09410

(b)

Indicator	Efficiency of electromechanical equipment	Power of electromechanical equipment	The number of equipment	Specific heat capacity of ore	Temperature difference between ore and air	Surface area of filling body	The number of worker at the working face	Daily gunpowder consumption
C^+	0.00187	0.00187	0.00187	0.00187	0.04369	0.03828	0.01433	0.02147
C^-	0.00187	0.00187	0.00187	0.00187	0.19253	0.08843	0.02389	0.04739

equipment, the number of equipment, and specific heat capacity of ore.

4.2. Evaluation of Heat Damage Degree of Stope Heat Source. The evaluation of heat damage in deep stope is a problem that needs to consider many factors and multi-attribute decision-making. The TOPSIS [21] method is a comprehensive evaluation method for multi-objective decision-making. It seeks the "positive ideal solution" and "negative ideal solution" in the evaluation indicators by means of the multi-attribute decision-making problem, so as to sort the evaluation objects. The positive ideal solution is a kind of virtual optimal solution, in which each indicator value reaches the optimal value of the evaluation object. The negative ideal solution is the virtual worst solution, in which each indicator value reaches the worst value of the evaluation object. By calculating the Euclidean distance between each evaluation indicator and positive and negative ideal solutions, the closeness level is obtained, and the ranking and evaluation results are obtained. The specific evaluation method and calculation process are shown in Figure 4:

Table 10: Euclidean distance and closeness level.

Depth/m	D_i^+	D_i^-	Z_i^+	Sequence
-930 m	0.0414	0.3740	0.9003	1
-945 m	0.0411	0.3643	0.8986	2
-960 m	0.3780	0.0193	0.0486	3

Calculate the Euclidean distance between the decision object and the positive ideal solution and the negative ideal solution, and compare the closeness level and ranking of each middle sample of heat damage to the positive ideal solution to determine the level attribution. The results are shown in Tables 8–10. It can be seen from Table 10 that the closeness level of heat damage in the sub-levels of -930 and -945 is close to 1, and the degree of heat damage is small; the closeness level of heat damage in the sub-level of -960 is close to 0, and the degree of heat damage is more serious than that of the other two sub-levels. The main reason is that the water inflow in the sub-level of -960 is much larger than that in the other two sub-levels, and it can be seen from Section 3.1 that the water inflow accounts for the largest proportion in the thermal environment assessment indicator. In addition, the transportation distance of ore and the vertical depth of the downward flow of air flow in the sub-level of -960 are significantly higher than those of the other two sub-levels, which are also secondary factors that cannot be ignored. Therefore, the heat damage in this sub-level is extremely serious. The closeness value of the sub-level of -945 and -930 has little difference, but there is a big difference between the closeness values of the sub-level of -960. It can be seen that the degree of thermal damage does not increase linearly with the increase of depth. It is the result of the comprehensive influence of various thermal environment evaluation indicator factors.

5. Conclusions

(1) Through monitoring and analyzing the thermal environment of deep stope in Sanshandao Gold Mine, the heat sources in stope area are divided into eight categories: surrounding rock heat release, underground water heat release, air compression heat release, electromechanical equipment heat release, ore transport process heat release, hydration heat release of the filling body, personnel heat release, and blasting heat release. Through the calculation of ambient temperature growth, quantitatively characterize the change of stope ambient temperature caused by heat release, and analyze the proportion structure of heat release in every stope. The heat release of surrounding rock and electromechanical equipment accounts for about 80% -90% of total heat release. Therefore, the prevention and control of stope heat damage should focus on these heat sources

(2) According to the theoretical formula of heat release from the heat source, 17 secondary evaluation indicators of thermal environment of deep stope are sorted out, specifically including the excavation face length, the roadway perimeter, the initial temperature of surrounding rock, the average temperature of air flow in the roadway, the mass flow of the air flow, the water inflow in the roadway, the initial temperature of water, the final temperature of the water, the distance between air inlet and bottom well elevation, the power of electromechanical equipment, the efficiency of electromechanical equipment, the number of equipment, the specific heat capacity of ore, the temperature difference between the ore and the air, the surface area of the filling body during one-time filling, the number of worker at the working face, and the daily gunpowder consumption at the operating site. EWM is used to calculate the weights of 17 evaluation indicators affecting the thermal environment, and the ranking of the evaluation factors that affect the thermal environment of the stope in the deep shaft roadway in the Sanshandao mining area in a single excavation working face is clarified. Among them, the influence weight of water inflow is the largest, followed by the temperature difference between ore and air, electromechanical equipment, and so on

(3) The TOPSIS method is used to predict the ranking of the heat damage in the three sub-levels of the stope. The results show that the heat damage in the sub-level of -960 is more serious than that in the sub-level of -930 and -945. It is necessary to strengthen the heat damage prevention measures of the stope, increase the number of air ducts, air flow mass flow, and reasonably arrange workers' working time to ensure the safe mining and working efficiency of the stope

Data Availability

The data used to support the findings of this study are included within the article.

Conflicts of Interest

The authors declare that there are no conflicts of interest regarding the publication of this paper.

Acknowledgments

The work was supported by the National Natural Science Foundation of China (Grant No.52074021), Key Research Development Program of Shandong Province (2019SDZY05) and the Fundamental Research Funds for the Central University (FRF-GF-20-01B).

References

[1] X. B. Li, J. Zhou, S. F. Wang, and B. Liu, "Review and exploration of deep solid resource exploitation," *The Chinese Journal of Nonferrous Metals*, vol. 27, no. 6, pp. 1236–1262, 2017.

[2] Q. Han, Y. Zhang, K. Li, and S. Zou, "Computational evaluation of cooling system under deep hot and humid coal mine in China: a thermal comfort study," *Tunnelling and Underground Space Technology*, vol. 90, pp. 394–403, 2019.

[3] M. F. Cai, D. L. Xue, and F. H. Ren, "Current status and development strategy of metal mines," *Chinese Journal of Engineering*, vol. 41, no. 4, 426 pages, 2019.

[4] P. G. Ranjith, J. Zhao, M. Ju, R. V. De Silva, T. D. Rathnaweera, and A. K. Bandara, "Opportunities and challenges in deep mining: a brief review," *Engineering*, vol. 3, no. 4, pp. 546–551, 2017.

[5] X. A. Peng, A. Di, A. Gz, and B. Hl, "New criterion for the spalling failure of deep rock engineering based on energy release," *International Journal of Rock Mechanics and Mining Sciences*, vol. 148, article 104943, 2021.

[6] M. C. He, P. Y. Guo, X. Q. Chen, L. Meng, and Y. Y. Zhu, "Research on characteristics of high-temperature and control of heat-harm of Sanhejian coal mine," *Chinese Journal of Rock Mechanics and Engineering*, vol. 29, no. S1, pp. 2593–2957, 2010.

[7] P. Roghanchi and K. C. Kocsis, "Challenges in selecting an appropriate heat stress index to protect workers in hot and humid underground mines," *Safety and Health at Work*, vol. 9, no. 1, pp. 10–16, 2018.

[8] Y. Y. Cui, K. Li, G. D. Mei, Y. Lu, and Y. X. Li, "Research progress of analysis and control technology of heat stress in deep mine," *Nonferrous Metals*, vol. 73, no. 2, pp. 128–134, 2021.

[9] S. O. Park, J. H. Roh, and K. Jin, "A study on evaluation of thermal environment using heat stress indices for deep coal mine in Korea," *Annales Medicinae Experimentalis et Biologiae Fenniae*, vol. 24, no. 2, pp. 166–175, 2014.

[10] W. H. Wang, Y. Wang, C. F. Du, and C. Y. Li, "Optimization of cooling method for deep shaft based on multi-objective decision," *Mining R & D*, vol. 41, no. 3, pp. 154–158, 2021.

[11] J. N. Gao, F. L. Wu, and W. F. Li, "Application of least square method based optimal combined weight model in comfort evaluation of mine environment," *Safety and Environmental Engineering*, vol. 27, no. 5, pp. 177–183, 2020.

[12] D. Y. Wei, C. F. Du, Y. F. Lin, B. M. Chang, and Y. Wang, "Thermal environment assessment of deep mine based on analytic hierarchy process and fuzzy comprehensive evaluation," *Case Studies in Thermal Engineering*, vol. 19, article 100618, 2020.

[13] S. Z. Luo, W. Z. Liang, and G. Y. Zhao, "Likelihood-based hybrid ORESTE method for evaluating the thermal comfort in underground mines," *Applied Soft Computing*, vol. 87, article 105983, 2020.

[14] H. W. Zhang, S. Xin, and C. Z. Jia, "The research on evaluation index system of mine thermal environment," *Advanced Materials Research*, vol. 962-965, pp. 1106–1111, 2014.

[15] R. Anderson and E. D. Souza, "Heat stress management in underground mines," *International Journal of Mining Science and Technology*, vol. 27, no. 4, pp. 651–655, 2017.

[16] Z. Zhou, Y. Cui, L. Tian, J. Chen, and P. Hu, "Study of the influence of ventilation pipeline setting on cooling effects in high-temperature mines," *Energies*, vol. 12, no. 21, p. 4074, 2019.

[17] M. C. He and M. Xu, "Research and development of HEMS cooling system and heat-harm control in deep mine," *Chinese Journal of Rock Mechanics and Engineering*, vol. 7, pp. 1353–1361, 2008.

[18] X. Nie, X. Wei, X. Li, and C. Lu, "Heat treatment and ventilation optimization in a deep mine," *Advances in Civil Engineering*, vol. 2018, Article ID 1529490, 2018.

[19] P. Guo, Y. Su, D. Pang, Y. Wang, and Z. Guo, "Numerical study on heat transfer between airflow and surrounding rock with two major ventilation models in deep coal mine," *Arabian Journal of Geosciences*, vol. 13, no. 16, p. 756, 2020.

[20] B. Wtwa, B. Shla, W. A. Yin, A. Cfy, A. Yfc, and C. Cms, "Thermal stability and exothermic behavior of imidazole ionic liquids with different anion types under oxidising and inert atmospheres," *Journal of Molecular Liquids*, vol. 343, article 117691, 2021.

[21] S. Kusi-Sarpong, C. Bai, J. Sarkis, and X. Wang, "Green supply chain practices evaluation in the mining industry using a joint rough sets and fuzzy TOPSIS methodology," *Resources Policy*, vol. 46, pp. 86–100, 2015.